Self-starting harmonic mode-locked Tm-Bi co-doped germanate fiber laser with carbon nanotube-based saturable absorber

N. Saidin[1,2], D. I. M. Zen[1,3], S. S. A. Damanhuri[1,2*], S. W. Harun[1,2], H. Ahmad[1], F. Ahmad[1,2], K. Dimyati[3], A. Halder[4], M. C. Paul[4], M. Pal[4], and S. K. Bhadra[4]**

[1]*Photonics Research Centre, University of Malaya, 50603 Kuala Lumpur, Malaysia*

[2]*Department of Electrical Engineering, Faculty of Engineering, University of Malaya, 50603 Kuala Lumpur, Malaysia*

[3]*Department of Electrical and Electronic Engineering, National Defense University of Malaysia, Kem Sungai Besi, 57000 Kuala Lumpur, Malaysia*

[4]*Fiber Optics and Photonics Division, Central Glass and Ceramic Research Institute, CSIR, Kolkata, India*

*Corresponding author: swharun@um.edu.my; **corresponding author: paulmukul@hotmail.com

Received January 8, 2013; accepted February 25, 2013; posted online April 24, 2013

We report a ring cavity passively harmonic mode-locked fiber laser using a newly developed thulium-bismuth co-doped fiber (TBF) as a gain medium in conjunction with a carbon nanotube (CNT)-based saturable absorber. The TBF laser generates a third harmonic mode-locked soliton pulse train with a high repetition rate of 50 MHz and a pulse duration of 1.86 ps. The laser operates at 1 901.6 nm with an average power of 6.6 mW, corresponding to a pulse energy of 0.132 nJ, at a 1 552 nm pump power of 723.3 mW.

OCIS codes: 320.0320, 140.0140.

doi: 10.3788/COL201311.063201.

Carbon nanotubes (CNTs) have gained tremendous attention because of their excellent electrical and optical properties and are used in various high performance electronic and photonic devices[1]. In particular, the unique nonlinear optical properties of CNTs make them ideal for implementation in a wide range of photonic devices, such as saturable absorbers (SAs)[1,2], ultrafast optical switches[3], and wavelength converters[4]. CNTs are known to provide distinctive advantages because of their ultra-fast recovery times and wide absorption bandwidth compared with their semiconductor-based counterparts[1]. Several studies have recently reported the use of CNT-based SAs for the implementation of Q-switched or mode-locked lasers. Aside from CNTs, graphene-based SAs may also be used for mode-locking applications[5−8]. Graph ene-based SAs have recovery times comparable with those of CNTs and feature wavelength-independent absorption, thereby allowing wide-band operation. Furthermore, most graph ene-based SAs can be applied in 1 550- and 1 060-nm wavelength applications using erbium (Er)- or ytterbium (Yb)-doped fiber gain media, respectively. However, CNT technology is more advanced than graph ene-based technology and device preparation in the former is simpler to perform than that in the latter.

2-μm pulsed lasers have also drawn significant research interest because of their usefulness in various applications, such as medicine, lidar, and remote sensing[9,10]. However, only a few mode-locked oscillators based on thulium (Tm)-doped fibers have been reported. For instance, Nelson *et al.* demonstrated a nonlinear polarization rotation (NPR)-based mode-locked Tm fiber laser with 500-fs pulse generation[11]. Sharp *et al.* reported a semiconductor SA mirror-based Tm fiber laser with 190-fs pulses[12]. Engelbrecht *et al.* recently reported a laser with grating-based dispersion compensation and double-clad Tm-doped fibers operated in the stretched pulse regime[13] with pulse energies of up to 4.3 nJ and dechirped pulse durations of approximately 300 fs.

We previously generated a broadband amplified spontaneous emission source operating in the 1 880-nm wavelength region using a Tm-bismuth co-doped fiber (TBF)[14]. The present study demonstrates a mode-locked TBF laser (TBFL) using a similar TBF in conjunction with a simple and low-cost CNT-based SA. The SA is constructed by sandwiching a single-walled CNT-polyethylene oxide (CNT-PEO) film fabricated using an evaporation technique between two fiber connectors.

The SA was fabricated using single-walled/double-walled CNTs with outer diameters of 1–2 nm, purity of $> 99\%$, and lengths of 3–30 μm. Briefly, 250 mg of the CNTs was added to 400 mL of sodium dedocyl sulfate (SDS) solution in deionized water at 1% concentration prior to sonication for 30 min at 50 W. Dispersion of single-walled CNTs in the solution was achieved ultrasonically with the aid of SDS. The solution was centrifuged at 1 000 rpm to remove large particles of undispersed CNTs and obtain a stable dispersed suspension. The CNT-PEO composite was prepared by thoroughly mixing 1.8 mL of the dispersed CNT suspension containing 1.125 mg of solid CNTs into a solution of 1 g of PEO (average molecular weight of 1×10^6 g/mol) in deionized water. The CNT-PEO composite was cast onto a glass Petri dish and kept inside a vacuum oven at 60 °C for 48 h to form a thin film of approximately 50 μm. The SA was fabricated by cutting a small piece of the prepared film (2×2 (mm)) and sandwiching it between two fiber connector/physical contact (FC/PC) fiber connectors after deposition of index-matching gel onto the fiber ends. Figures 1(a) and (b) show images of the film pasted onto a fiber ferule and the constructed SA, respectively. The insertion losses of the SA were approximately 6 and 4 dB at wavelengths of 1 550 and 1 901.6 nm, respectively.

A schematic of our mode-locked TBFL is shown in Fig. 2. The fiber laser was constructed using a simple ring cavity. A 5-m-long TBF was used as the active medium and the fabricated CNT-based SA was used as a mode-locker. The TBF was fabricated in-house and had a circular cladding with core and cladding diameters of 7 and 125 μm, respectively. Electron probe microscopic analysis indicated that the dopant concentrations (wt.%) and compositions inside the core of the fabricated TBF were 0.35 Bi_2O_3, 0.9 Tm_2O_3, 3.0 Al_2O_3, and 4.0 GeO_2, which corresponded to a Bi/Tm ratio of 1:2. The numerical aperture (NA) and dispersion parameter of the fiber were approximately 0.24 and 30.3 ps/(nm·km), respectively. The TBF was pumped by a 1 552-nm Er-Yb co-doped fiber laser via a 1 550/980-nm wavelength division multiplexer. The operating wavelength of the proposed TBFL was determined by the fiber Bragg grating (FBG), which was connected to port 2 of the circulator so that the reflection from the FBG could be routed back into the laser cavity via port 3. The circulator was used to allow the light reflected from the FBG to oscillate in the ring cavity and ensure the unidirectional operation of the laser. The FBG used had a center wavelength of 1 901.6 nm, a 3-dB bandwidth of 1.5 nm, and a reflectivity of 99.6%. The ring cavity length was estimated to be approximately 13.9 m, which corresponded to a fundamental repetition rate of 14.6 MHz. The net dispersion was approximately –0.188 ps^2/km. The temporal characteristics of the laser output were monitored using a photo-detector (PD) combined with a real-time oscilloscope. The optical spectrum was

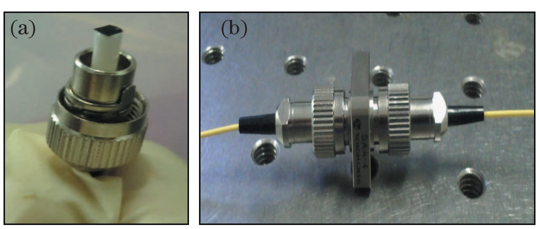

Fig. 1. CNT-PEO film-based SA. (a) Attachment of the film to the fiber ferrule and (b) integration of the CNT composite film into the laser cavity.

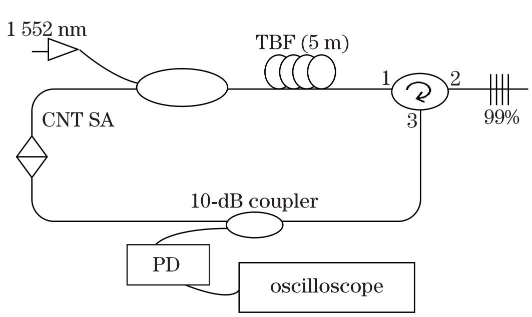

Fig. 2. Schematic of the proposed mode-locked TBFL.

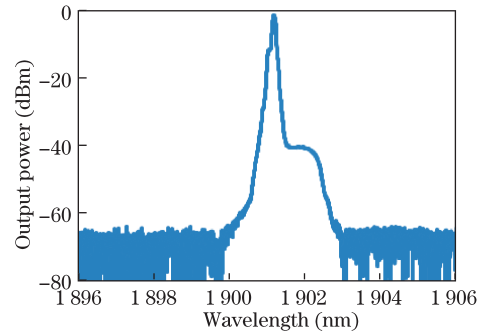

Fig. 3. Output spectrum of the proposed mode-locked TBFL at a 1552-nm pump power of 723.3 mW.

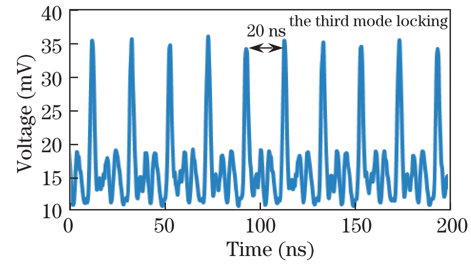

Fig. 4. Oscilloscope trace of the laser output at a pump power of 723.3 mW showing a pulse train with a repetition rate of 50 MHz.

measured using an optical spectrum analyzer.

The TBFL starts to lase at a threshold pump power of 421.5 mW during continuous wave (CW) operation. The laser always operates during CW operation in the absence of a SA in the cavity, and the operation is insensitive to the polarization state. As the CNT-based SA is incorporated in the laser cavity, the mode-locked laser self-startsat a 1 552-nm pump power of 613.4 mW without introducing disturbances to the intra-cavity fiber. The optical spectrum of the passively mode-locked laser is shown in Fig. 3. The mode-locked laser operates at a center wavelength of 1 901.6 nm, which coincides with a FBG wavelength at full-width at half-maximum (FWHM) of 0.32 nm. Considering that the laser operates in negative cavity dispersion mode, pulse generation may most probably be attributed to the soliton effect produced from the balance between the self-phase modulation and group velocity dispersion (GVD). Figure 3 shows that the typical Kelly sideband signature of deviation from the average soliton operation is not observed despite the anomaly of the net cavity dispersion. This finding is attributed to the longer soliton length ($z_{\text{sol.}} = 23.58$ km) compared with the cavity length (13.9 m). The soliton length is calculated using $z_{\text{sol.}} = \frac{\pi}{2}\frac{\tau_0^2}{|\beta_2|}$, where τ_0 and β^2 are the pulse duration and GVD, respectively.

Figure 4 shows a pulse train from the mode-locked TBFL recorded by an oscilloscope. The time interval is approximately 20 ns, which corresponds to a repetition rate of 50 MHz. Multiple pulses are generated as identified in the pulse train, which is attributed to energy quantization. The high repetition rate obtained is attributed to multiple pulses circulating inside the cavity that generate the harmonic mode-locked fiber laser.

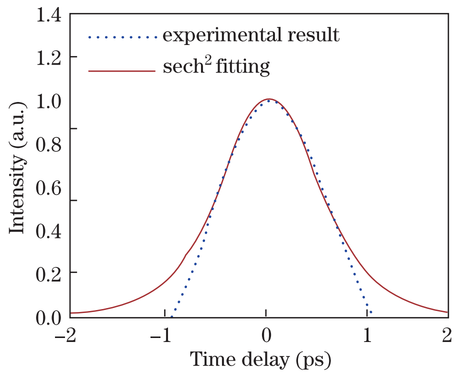

Fig. 5. (Color online) Autocorrelation trace of output pulses with FWHM of 1.68 ps.

Besides gain competition between multiple pulses, the major factors that influence this phenomenon are related to the peak-power limiting effect of the laser cavity. The generated mode-locked laser operates in the third harmonic mode from the fundamental mode, which proves that the proposed CNT-based SA is able to operate efficiently in the ring TBFL. Figure 5 shows a typical second harmonic generation autocorrelation trace for the third harmonic mode-locked laser. The pulse duration at FWHM calculated by applying sech^2 fitting to the output curve is approximately 1.68 ps. The calculated time bandwidth product (TBP) is 139, which shows that the output pulse is highly chirp. The higher TBP is attributed to the remaining dispersion, which occurs outside the cavity from the 2.7-m-long SMF-28 fiber to the autocorrelator, and the resonant CNT dispersion. The average output power increases with increase in 1 552-nm pump power and pulse energy. The average output power at a threshold pump power of 613.4 mW is 3.3 mW, which corresponds to a pulse energy of 0.066 nJ. At a higher pump power of 723.3 mW, the output power is 6.6 mW, which corresponds to a pulse energy of 0.132 nJ. The wavelength operation of the mode-locked fiber laser may be expected to be tunable when the resonance wavelength of the FBG is shifted. Optimization of the insertion loss and refractive index of the TBF- and CNT-based SA can improve the quality of pulses and repetition rate.

In conclusion, a third harmonic mode-locked fiber laser is demonstrated using a newly developed TBF- and CNT-based SA in an all-fiber configuration. The TBF is pumped by a 1 552-nm fiber laser operating at 1 901.6 nm with the assistance of a FBG. The SA is assembled by sandwiching a CNT-PEO film fabricated using single-walled/double-walled CNTs with outer diameters of 1–2 nm. The proposed laser generates a soliton pulse train with a repetition rate of 50 MHz and pulse duration of 1.68 ps. The laser has an average power of 6.6 mW, which corresponds to a pulse energy of 0.132 nJ, at a 1 552-nm pump power of 723.3 mW.

This work was supported by Ministry of Higher Education (MOHE) under the Exploratory Research Grant Scheme (ERGS) (No. ER012-2012A) and the University of Malaya under a Pangurusan Penyelidikan Pascasiswazah (PPP) Grant (No. PV030/2012A).

References

1. F. Wang, A. G. Rozhin, V. Scardaci, Z. Sun, F. Hennrich, I. H. White, W. I. Milne, and A. C. Ferrari, Nat. Nanotechnol. **3,** 738 (2008).
2. Z. Sun, A. G. Rozhin, F. Wang, T. Hasan, D. Popa, W. O'Neill, and A. C. Ferrari, Appl. Phys. Lett. **95,** 253102 (2009)
3. Y. W. Song, S. Y. Set, and S. Yamashita, in *Proceedings of Conference on Lasers and Electro Optics* (*CLEO 2006*) CMA4 (2006).
4. K. K. Chow, S. Yamashita, and S. Y. Set, Opt. Lett. **35,** 2070 (2010).
5. H. Zhang, Q. Bao, D. Tang, L. Zhao, and K. Loh, Appl. Phys. Lett. **95,** 141103 (2009).
6. H. Zhang, D. Tang, L. Zhao, Q. Bao, and K. Loh, Opt. Express **17,** 17630 (2009).
7. Z. Zheng, C. Zhao, S. Lu, Y. Chen, Y. Li, H. Zhang, and S. Wen, Opt. Express **20,** 23201 (2012).
8. Y. K. Yap, R. M. De La Rue, C. H. Pua, S. W. Harun, and H. Ahmad, Chin. Opt. Lett. **10,** 041405 (2012).
9. J. Wu, Z. Yao, J. Zong, and S. Jiang, Opt. Lett. **32,** 638 (2007).
10. S. W. Harun, N. Saidin, S. S. A. Damanhuri, H. Ahmad, A. Halder, M. C. Paul, S. Das, M. Pal, and S. K. Bhadra, Laser Phys. Lett. **9,** 50 (2012).
11. L. E. Nelson, E. P. Ippen, and H. A. Haus, Appl. Phys. Lett. **67,** 19 (1995).
12. R. C. Sharp, D. E. Spock, N. Pan, and J. Elliot, Opt. Lett. **21,** 881 (1996).
13. M. Engelbrecht, F. Haxsen, A. Ruehl, D. Wandt, and D. Kracht, Opt. Lett. **33,** 690 (2008).
14. A. Halder, M. C. Paul, S. W. Harun, S. M. M. Ali, N. Saidin, S. S. A. Damanhuri, H. Ahmad, S. Das, M. Pal, and S. K. Bhadra, IEEE Photon. J. **4,** 2176 (2012).